AIP | Journal of Applied Physics

Elasticity and sound velocities of polycrystalline Mg3Al2(SiO4)3 garnet up to 20GPa and 1700K

Yongtao Zou, Tetsuo Irifune, Steeve Gréaux, Matthew L. Whitaker, Toru Shinmei et al.

Citation: J. Appl. Phys. **112**, 014910 (2012); doi: 10.1063/1.4736407
View online: http://dx.doi.org/10.1063/1.4736407
View Table of Contents: http://jap.aip.org/resource/1/JAPIAU/v112/i1
Published by the American Institute of Physics.

Elasticity and sound velocities of polycrystalline $Mg_3Al_2(SiO_4)_3$ garnet up to 20 GPa and 1700 K

Yongtao Zou,[1,2,a)] Tetsuo Irifune,[1] Steeve Gréaux,[1] Matthew L. Whitaker,[3] Toru Shinmei,[1] Hiroaki Ohfuji,[1] Ryo Negishi,[1] and Yuji Higo[4]
[1]*Geodynamics Research Center, Ehime University, Matsuyama 790-8577, Japan*
[2]*Graduate School of Science and Engineering, Ehime University, Matsuyama 790-8577, Japan*
[3]*Mineral Physics Institute, State University of New York at Stony Brook, New York 11794-2100, USA*
[4]*Japan Synchrotron Radiation Institute, Hyogo 679-5198, Japan*

(Received 6 February 2012; accepted 7 June 2012; published online 13 July 2012)

Elastic wave velocities of synthetic polycrystalline $Mg_3Al_2(SiO_4)_3$ garnet have been successfully measured to 20 GPa and temperatures up to 1700 K by ultrasonic interferometry combined with energy-dispersive synchrotron x-ray diffraction in a Kawai-type multi-anvil apparatus. Compressional (*Vp*) and shear (*Vs*) wave velocities as well as the adiabatic bulk (*Ks*) and shear (*G*) moduli exhibit monotonic increase with increasing pressure and decrease with increasing temperature, respectively. Two-dimensional (*P-T*) linear fittings of the present data yield the following parameters: $K_{S0} = 170.0(2)$ GPa, $\partial Ks/\partial P = 4.51(2)$, $\partial Ks/\partial T = -0.0170(1)$ GPa/K, $G_0 = 93.2(1)$ GPa, $\partial G/\partial P = 1.51(2)$, and $\partial G/\partial T = -0.0107(1)$ GPa/K, which is in good agreement with the earlier results by Brillouin scattering and/or ultrasonic measurements at relatively low *P-T* conditions. The observed linear pressure and temperature dependence in both *Vp* and *Vs* is in contrast to the non-linear behavior of *Vp* and *Vs* for majorite garnet with the pyrolite composition, in particular for *Vs*. © *2012 American Institute of Physics*. [http://dx.doi.org/10.1063/1.4736407]

I. INTRODUCTION

Garnets, as an important and attractive class of materials, are widely used as gemstones, laser host materials, microwave optical elements, abrasives, water jet cutters, pigments for ceramic industry as well as a substitution of silica sand in sand blasting because of its excellent physical prosperities, such as high thermochemical stability, good mechanical properties, and excellent optical/magnetic properties.[1–3] Silicate garnets are also considered important constituents in the Earth's upper mantle and mantle transition zone, comprising 40% by volume of the pyrolite composition. The mantle transition zone is sandwiched by two seismic discontinuities, i.e., at depths between 410 km (~13.5 GPa) and 660 km (~24 GPa).[4–6] Elastic properties and acoustic velocities of garnets are of great interest and importance not only because of their geophysical relevance but also due to their myriad technological applications.[7,8]

$X_3Y_2(ZO_4)_3$ garnets, centered cubic lattice (space group $Ia\bar{3}d$), display dodecahedral (X), octahedral (Y), and tetrahedral (Z) crystallographic sites. This unique behavior makes the garnet structure flexible in accommodating various chemical substitutions with different ionic radii, suggesting that garnets could be composition diverse where $X = Mg^{2+}$, Fe^{2+}, Ca^{2+}, Mn^{2+}, Y^{3+}; $Y = Al^{3+}$, Fe^{3+}, Cr^{3+}; $Z = Al^{3+}$, Fe^{3+}, Si^{4+}, Ti^{4+}. Chemical substitutions at octahedral and triangular dodecahedral sites may change the relative bond lengths/interatomic distances and angles, which will result in affecting their elastic properties and sound velocities.

Pyrope garnet with the composition of $Mg_3Al_2(SiO_4)_3$ is the magnesium end-member of garnets group, and therefore, its physical properties are of great significance. Elastic properties of $Mg_3Al_2(SiO_4)_3$ pyrope garnet for both single crystal and synthetic polycrystalline samples have been investigated by many scientists with different techniques, including ultrasonic interferometry, Brillouin scattering, and static compression methods.[8–15]

Earlier experimental study on the elasticity of polycrystalline $Mg_3Al_2(SiO_4)_3$ garnet has been carried out by Chen *et al.*[10] using ultrasonic interferometry techniques in a multi-anvil apparatus to 10 GPa at room temperature. Subsequently, static compression experiments of pyrope garnet were performed by Zhang *et al.*[14] in a diamond anvil cell (DAC) up to 33 GPa at room temperature. Afterwards, Conrad *et al.*[15] carried out Brillouin scattering experiments on a natural pyrope garnet at pressures up to 10 GPa and room temperature. However, the reported pressure derivative for bulk modulus $K' = 3.22$ showed a significantly discrepancy, as compared with those of previous studies.[8–15] Recently, Gwanmesia *et al.*[9] have studied the high-temperature elastic properties of synthetic polycrystalline $Mg_3Al_2(SiO_4)_3$ garnet to 1000 K and 0.3 GPa with a gas-medium apparatus. Moreover, high-temperature elasticity of single crystal pyrope garnet has been investigated to 800 °C at room pressure by Brillouin scattering.[9]

However, to date, direct measurements of the elastic properties of $Mg_3Al_2(SiO_4)_3$ pyrope garnet based on *in situ* high *P-T* experiments are still limited. Previous studies were carried out either at high temperature and ambient pressure or at high pressure and room temperature.[10–12,14] The recent simultaneous high-pressure and high-temperature study on the elasticity of polycrystalline $Mg_3Al_2(SiO_4)_3$ garnet was

a)Author to whom correspondence should be addressed. Electronic addresses: yongtaozou@yahoo.com.cn and yongtao@sci.ehime-u.ac.jp.

carried out to 9 GPa and 1000 °C using the ultrasonic interferometric techniques,[8] but these experimental *P-T* conditions are not accessible to the mantle conditions and/or do not cover its entire stability field proposed by Hirose *et al.*[16]

In addition, the previous studies on the elasticity, especially for their pressure and temperature dependences are not well constrained.[8–14] The pressure dependences of the bulk and shear modulus were measured using Brillouin spectroscopy by Conrad *et al.*[15] and Sinogeikin and Bass,[11] yielding values of $K_0' = 3.2$ and $G_0' = 1.4$ as well as $K_0' = 4.1(3)$ and $G_0' = 1.3(2)$, respectively. In contrast, the ultrasonic measurement experiment gave values of $K_0' = 5.3(4)$, $G_0' = 1.6(2)$,[10] and $K_0' = 3.9(3)$, $G_0' = 1.7(2)$ by Gwanmesia *et al.*[8,9] The pressure derivatives for the shear modulus from the previous studies are compatible, whereas those for the bulk modulus are not. Meanwhile, the temperature dependences of bulk and shear modulus were measured by Brillouin spectroscopy[12] and ultrasonic measurement,[8,9] giving values of $\partial K_S/\partial T = -0.0206(15)$ GPa/K and $\partial G/\partial T = -0.0101(8)$ as well as $\partial K_S/\partial T = -0.0140(20)$ GPa/K and $\partial G/\partial T = -0.0092(10)$, respectively. The temperature dependences of the shear modulus are also comparable to previous studies within uncertainties, whereas those of the bulk modulus show obvious disagreements.

It is thus of great geophysical/engineering importance to carry out further studies for $Mg_3Al_2(SiO_4)_3$ garnet at elevated pressures and temperatures to understand its elasticity/elastic wave velocities as well as some implications for other garnets such as $Y_3Al_2(AlO_4)_3$ (YAG) and $Y_3Fe_2(FeO_4)_3$ (YIG).

In this paper, we report the elastic properties of synthetic polycrystalline pyrope $Mg_3Al_2(SiO_4)_3$ garnet up to 20 GPa and 1700 K, equivalent to the middle part of the mantle transition zone, using ultrasonic interferometry combined with energy-dispersive synchrotron x-ray diffraction in a Kawai-type multi-anvil apparatus.

II. EXPERIMENTAL

Polycrystalline $Mg_3Al_2(SiO_4)_3$ pyrope sample was synthesized at 11 GPa and 1200 °C for 1.5 h from a homogeneous glass with pyrope composition using a Kawai-type multi-anvil apparatus at Geodynamics Research Center, Ehime University, Japan. The fine glass powder was dried in an oven and then enclosed in a Pt capsule with a wall thickness of 0.1 mm. Tungsten carbide cubic anvils with 8 mm truncation edge length are used as the second stage anvils of the high-pressure apparatus. The pressure medium was a semi-sintered (Mg, Co)O octahedron of 14 mm in edge. A cylindrical $LaCrO_3$ heater was put into the pressure medium. In this hot-pressed experiment, a special *P-T* path[8,17] was designed to relax intergranular stresses and to obtain a well-sintered sample. The synthetic sample with 2 mm both in diameter and length appeared to be translucent, well-sintered and free of visible macro-cracks. X-ray diffraction shows that the synthetic sample is a single phase of $Mg_3Al_2(SiO_4)_3$ pyrope, as shown in Fig. 1. It is also shown by SEM observations that the average grain size of the synthetic sample is about 2–3 μm with porosity of ~0.5%, which was evaluated by Archimedes' immersion method.

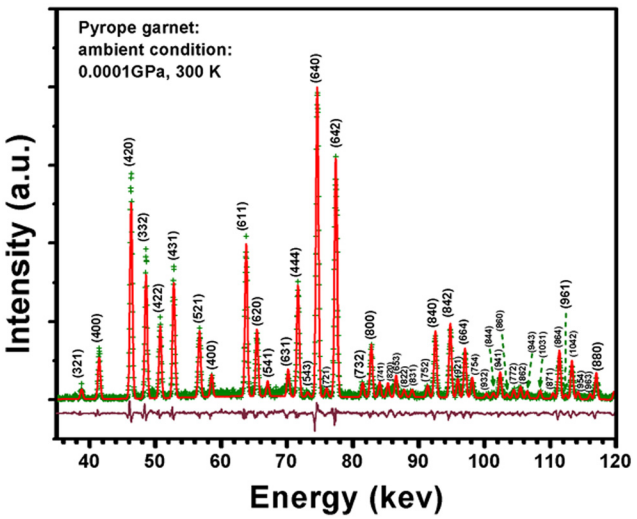

FIG. 1. Observed (cross) and fitted (line) x-ray diffraction pattern of the synthetic polycrystalline $Mg_3Al_2(SiO_4)_3$ garnet at ambient condition, which indicates that the synthetic garnet sample for the present ultrasonic measurements is a single phase of pyrope garnet. Residuals are shown at the bottom of the figure.

Elastic wave velocities of polycrystalline pyrope sample were measured at high pressure and high temperature using ultrasonic interferometric techniques in conjunction with energy-dispersive synchrotron x-ray diffraction in a Kawai-type multi-anvil apparatus at SPring-8 (Beamline BL04B1). Details of this experimental setup have been described by Higo *et al.*[18] A schematic illustration of the cell assembly used for *in situ* experiments is shown in Fig. 2, modified from Kono *et al.*[19] We used a rhenium foil tube heater, instead of graphite heater used by previous studies,[20–22] so that high *P-T* condition can be achieved. As is known,

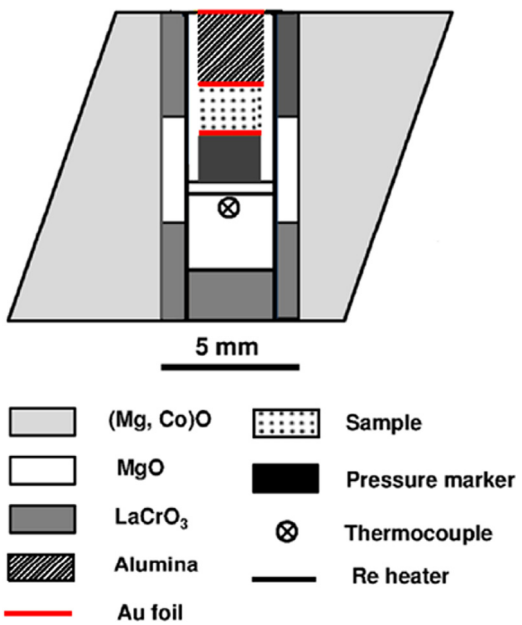

FIG. 2. Cross section of the cell assembly for *in situ* acoustic and x-ray measurements at high pressure and high temperature. Gold foils with thickness of 2 μm were inserted at both sides of the sample as markers of x-radiography image; Gold foils between buffer rod and sample, as well as buffer rod and WC anvil were used to improve the mechanical coupling.

graphite partially transforms to diamond at *P-T* condition above 15 GPa and 1500 K, leading to unstable heating and/or eventual termination of the heating. Temperature was monitored with a $W_{97}Re_3$-$W_{75}Re_{25}$ thermocouple located at the opposite side of the sample for measuring the temperature comparable to the center position of the sample. $LaCrO_3$ sleeve was used as a thermal insulator, and MgO window was placed in $LaCrO_3$ sleeve for obtaining x-radiography image and x-ray diffraction of the sample. Both surfaces of the hot-pressed sample were well-polished using 1 μm diamond paste to minimize the loss of acoustic energy. A $LiNbO_3$ transducer (10° rotated Y-cut), which produces both longitudinal and transverse acoustic signals, was used to generate and receive the ultrasonic signals. The transducer was mounted with a special high temperature epoxy on a polished surface of a WC anvil cube, which was diagonal to the anvil top contacted with Al_2O_3 buffer rod. At increasing pressures, the transducer remains free of stress, because it is located in the gap between the first-stage anvils and the second-stage cubes. The polished surface of the sample was connected to an alumina (Al_2O_3) buffer rod via a gold film with a thickness of 2 μm to improve mechanical connection. The other surface of the sample was contacted with pressure marker of Au + NaCl + BN disk through the same gold film.

Travel times for *P*- and *S*- waves were simultaneously determined by a pulse echo overlap using a transfer function method[23,24] with standard deviation of 0.2 ~ 0.4 ns. The sample length at high pressure and high temperature was directly determined by x-radiography image. The precision of this direct measurement of sample length was about 0.2 ~ 0.4%.[18,19,24,25]

In this experiment, we performed seven heating/cooling cycles at different pressures and temperatures up to 20 GPa and 1700 K. We first increased pressure to ~18 GPa, and then temperature was increased to 1100 K at the fixed press load to relax the deviatoric stress imposed on the sample upon compression. The sharp diffraction peaks for garnet sample and pressure marker after heating indicated that the residual stress was substantially reduced by this procedure, as compared to those before heating. After annealing at the desired temperature of 1100 K for about ~20 min, we measured the ultrasonic travel time, sample length, and x-ray diffraction patterns of both the sample and pressure marker. The same data collections have been done at every 200 K on decreasing temperature down to room temperature of 300 K. Then, the pressure was increased by increasing the press load and the same measurements were conducted after heating to the desired temperature of 1100 K upon decreasing temperature. This experimental procedure was repeatedly for several times at *P-T* conditions up to 20 GPa and 1700 K. Additional measurements have also been conducted on release of pressure with the same procedure as adopted in the process of increasing pressure. Based on the phase relations for pyrope garnet by Hirose *et al.*,[16] it is obviously seen that our sound velocities measurement has been done within the stability field of pyrope at pressures up to ~20 GPa and temperatures up to 1700 K, equivalent to the middle part of the mantle transition zone.

III. RESULTS AND DISCUSSION

To understand the nature of the synthetic $Mg_3Al_2(SiO_4)_3$ pyrope garnet, the microstructure/morphology, grain size, and unit cell parameters/density were analyzed by TEM-SAED, XRD, Raman spectroscopy, and Archimedes draining method. X-ray diffraction and Raman spectroscopy both show that the polycrystalline sample is a uniform phase composition of pyrope ($Mg_3Al_2Si_3O_{12}$). Fig. 3(a) shows a TEM image of the recovered sample after our ultrasonic measurements, showing that well-sintered and equilibrium textures formed with the average grain size of about 1–2 μm, and without any observable porosity, secondary phases, and/or micro-cracks. The corresponding SAED pattern obtained

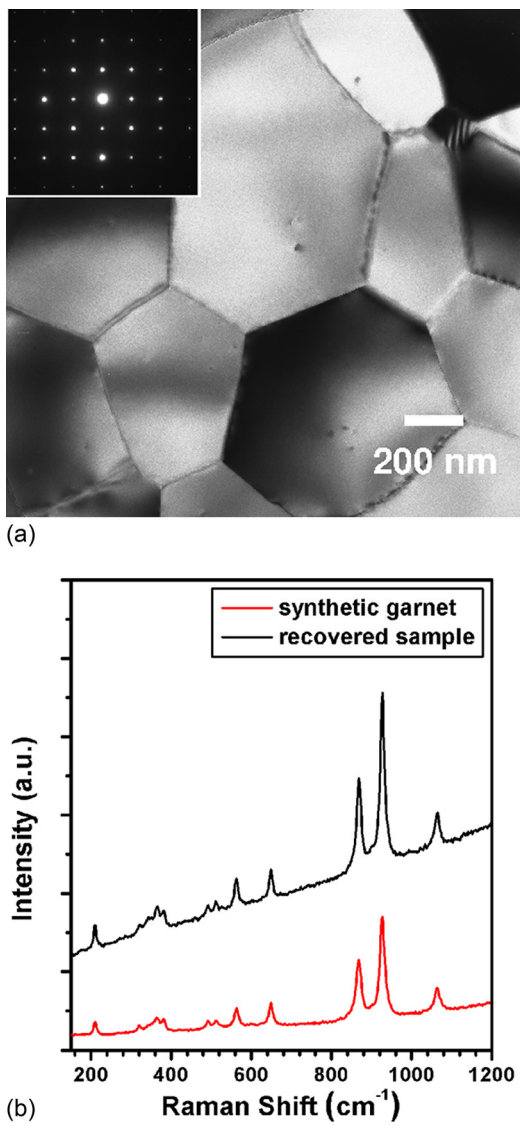

FIG. 3. (a). TEM image showing the microstructure of the polycrystalline $Mg_3Al_2(SiO_4)_3$ pyrope garnet recovered from the present sound velocity measurements at pressures up to 20 GPa and temperatures up to 1700 K. The average grain size of the recovered sample observed from TEM is about 1-2 μm. The corresponding selected area electron diffraction (SAED) pattern, as an up-left inset, proves that the obtained sample is cubic. (b). Representative Raman spectra collected from the present $Mg_3Al_2(SiO_4)_3$ pyrope sample at ambient condition before compression (bottom) and after decompression (upper).

from one grain, as an up-left inset, shows that the obtained sample is cubic.

Energy-dispersive x-ray diffraction patterns obtained at the entire *P-T* conditions show that the garnet sample consists of a single pyrope garnet phase, and there is no other phase observed and/or phase transformations happen throughout our ultrasonic measurements. Fig. 3(b) presents a typical Raman spectra collected from the present experiment at ambient condition before compression and after decompression, which further proves that no other phase occurs and/or phase transitions happen during our sound velocities measurement.

The lattice parameter and unit cell volume at different *P-T* conditions were determined from the *in situ* x-ray diffraction data. The corresponding densities can be calculated by using the molecular weight divided by the molar volume, which is shown in Table I. From the travel times and the sample length data (Table I), *P*- and *S*-wave velocities were plotted as a function of pressure at room temperature together with previous studies shown in Fig. 4. Both compressional (*Vp*) and shear (*Vs*) wave velocities of this study show an excellent agreement with previous study by Gwanmesia *et al.*[8] The shear wave velocity (*Vs*) is also consistent with the result of Sinogeikin and Bass[11] and Chen *et al.*,[10] while the compressional wave velocity (*Vp*) is slightly larger and smaller than that of Sinogeikin and Bass[11] and Chen *et al.*[10] at relatively high pressure region, respectively. The possible reasons may be due to the stress and/or pressure calibration.

The longitudinal ($L = \rho Vp^2$) and shear ($G = \rho Vs^2$) moduli are calculated from *P* and *S* wave velocities and densities, as shown in Table II. All the longitudinal and shear moduli data in the entire *P-T* range are fitted simultaneously using the third-order finite strain equations combined with the previous study by Wang *et al.*,[13] which yields the optimized K_S

TABLE I. Experimental conditions and results for polycrystalline $Mg_3Al_2(SiO_4)_3$ garnet.

T (K)	V_0 (Å^3)	V/V_0	ρ (g/cm^3)	Vp (km/s)	V_S (km/s)	Ks (GPa)	G (GPa)	P (GPa)
300	1440.41(11)	0.9585(1)	3.7183(3)	9.63(2)	5.32(1)	204.9(12)	105.1(4)	7.86(5)
300	1426.70(14)	0.9494(1)	3.7541(4)	9.78(2)	5.37(1)	214.6(13)	108.2(4)	9.84(6)
300	1409.40(15)	0.9379(1)	3.8002(4)	9.95(2)	5.43(1)	226.6(14)	112.1(4)	12.48(8)
300	1398.64(7)	0.9307(1)	3.8294(2)	10.06(2)	5.47(1)	234.3(19)	114.7(6)	14.21(12)
300	1392.57(13)	0.9267(1)	3.8461(4)	10.11(2)	5.50(1)	238.5(12)	116.2(4)	15.21(8)
300	1389.59(8)	0.9247(1)	3.8543(2)	10.15(2)	5.51(1)	241.1(19)	117.0(6)	15.71(12)
300	1386.32(17)	0.9225(1)	3.8634(5)	10.18(4)	5.52(2)	243.5(31)	117.8(9)	16.27(21)
500	1443.31(11)	0.9604(1)	3.7109(3)	9.60(1)	5.28(1)	203.6(10)	103.5(3)	8.26(4)
500	1431.05(9)	0.9523(1)	3.7427(2)	9.73(2)	5.33(1)	212.3(13)	106.3(4)	10.03(6)
500	1412.80(8)	0.9401(1)	3.7910(2)	9.90(2)	5.40(1)	224.5(17)	110.5(5)	12.80(10)
500	1401.65(10)	0.9327(1)	3.8212(3)	10.02(2)	5.44(1)	232.7(14)	113.2(4)	14.62(9)
500	1395.63(13)	0.9287(1)	3.8377(4)	10.08(2)	5.47(1)	237.1(16)	114.7(5)	15.62(11)
500	1392.76(13)	0.9268(1)	3.8456(3)	10.11(3)	5.48(1)	239.2(21)	115.5(6)	16.11(14)
500	1390.91(16)	0.9256(1)	3.8507(5)	10.13(3)	5.49(1)	240.5(21)	115.9(6)	16.43(15)
700	1446.96(14)	0.9628(1)	3.7015(4)	9.58(2)	5.26(1)	203.4(14)	102.5(4)	9.01(6)
700	1435.20(7)	0.9550(1)	3.7318(2)	9.71(2)	5.31(1)	211.8(13)	105.2(4)	10.72(6)
700	1416.53(8)	0.9426(1)	3.7810(2)	9.90(2)	5.38(1)	224.6(15)	109.5(5)	13.59(9)
700	1404.77(12)	0.9348(1)	3.8127(3)	10.02(2)	5.43(1)	233.2(13)	112.4(4)	15.50(9)
700	1399.76(11)	0.9314(1)	3.8263(3)	10.07(2)	5.45(1)	236.7(18)	113.7(5)	16.33(13)
700	1397.37(9)	0.9299(1)	3.8329(2)	10.10(3)	5.46(1)	238.9(20)	114.3(6)	16.74(14)
700	1395.30(23)	0.9285(2)	3.8386(6)	10.12(2)	5.47(1)	240.2(21)	114.8(6)	17.09(15)
900	1450.69(22)	0.9653(1)	3.6920(6)	9.56(2)	5.24(1)	202.8(12)	101.2(4)	9.58(6)
900	1440.19(13)	0.9583(1)	3.7189(3)	9.68(2)	5.28(1)	210.2(16)	103.7(5)	11.11(8)
900	1420.30(13)	0.9451(1)	3.7710(3)	9.88(2)	5.36(1)	224.0(16)	108.3(5)	14.18(10)
900	1408.10(15)	0.9370(1)	3.8037(4)	10.01(2)	5.41(1)	232.6(12)	111.3(4)	16.16(9)
900	1403.24(14)	0.9338(1)	3.8168(4)	10.06(2)	5.43(1)	236.3(19)	112.5(6)	16.98(14)
900	1400.99(13)	0.9323(1)	3.8230(3)	10.08(4)	5.44(2)	237.9(29)	113.1(8)	17.36(22)
900	1399.29(26)	0.9311(2)	3.8276(7)	10.10(3)	5.45(1)	239.4(21)	113.5(6)	17.65(16)
1100	1442.60(10)	0.9599(1)	3.7127(3)	9.68(2)	5.26(1)	210.5(17)	102.8(5)	11.91(10)
1100	1422.47(14)	0.9466(1)	3.7652(4)	9.88(2)	5.34(1)	224.4(16)	107.5(5)	15.03(11)
1100	1412.10(15)	0.9397(1)	3.7929(4)	9.99(2)	5.39(1)	232.0(15)	110.0(4)	16.73(11)
1100	1409.43(10)	0.9379(1)	3.8001(3)	10.02(2)	5.40(1)	233.7(16)	110.7(4)	17.18(12)
1100	1405.64(13)	0.9354(1)	3.8103(3)	10.06(2)	5.41(1)	236.9(19)	111.7(5)	17.82(15)
1100	1402.99(25)	0.9336(2)	3.8175(7)	10.09(3)	5.42(2)	238.6(24)	112.3(7)	18.28(18)
1300	1413.29(14)	0.9404(1)	3.7897(4)	10.01(2)	5.38(1)	233.5(14)	109.5(4)	17.78(11)
1300	1409.02(17)	0.9376(1)	3.8012(5)	10.05(2)	5.39(1)	236.2(17)	110.6(5)	18.50(14)
1300	1406.27(35)	0.9358(1)	3.8086(1)	10.08(3)	5.40(1)	238.6(22)	111.3(6)	18.98(18)
1500	1412.96(9)	0.9402(1)	3.7906(2)	10.04(3)	5.37(1)	236.2(20)	109.3(6)	19.08(16)
1500	1410.75(29)	0.9388(2)	3.7965(8)	10.06(3)	5.38(2)	237.5(23)	110.0(7)	19.46(19)
1700	1415.72(26)	0.9421(2)	3.7832(7)	10.02(5)	5.35(3)	235.8(39)	108.0(11)	19.86(34)

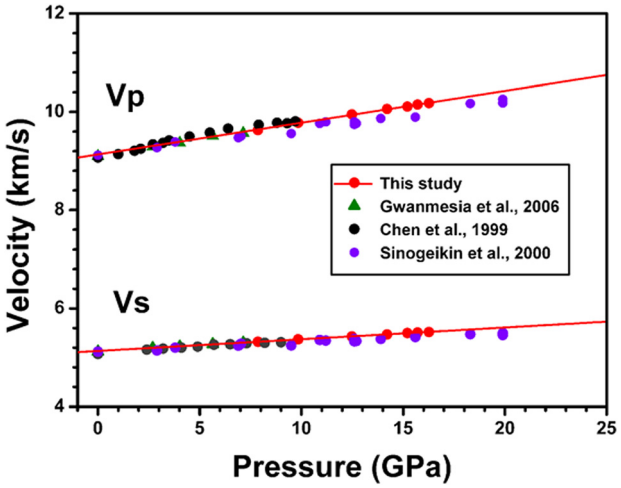

FIG. 4. Comparison of compressional (*Vp*) and shear (*Vs*) wave velocities of polycrystalline $Mg_3Al_2(SiO_4)_3$ pyrope garnet from this study with previous data (Refs. 8–11).

and K_S'. More details of the fitting procedures can be found in the previous studies.[17,26–28]

Using the fitted values of K_S and K_S', we have determined isothermal bulk modulus $K_{T0} \approx 169$ GPa with the formula of $Ks = K_T(1 + \alpha\gamma T)$, where the thermal expansivity: $\alpha_{(300\,K)} = 2.2(2) \times 10^{-5}\,K^{-1}$ and Grüneisen parameter $\gamma_0 = 1.15$ from Ref. 13. The obtained isothermal bulk modulus 169 GPa is in good agreement with the values of $K_{T0} \approx 171$ (2) (Ref. 14) and $K_{T0} \approx 167$ (4) (Ref. 8) within mutual uncertainties, respectively. The calculated $K_{S0}^{'} = 4.59$ is also consistent with previous study of $K_{S0}^{'} = 4.4(2)$.[14] No correction was made between $K_{S0}^{'}$ and $K_{T0}^{'}$ in this study, because the difference is significantly less than the uncertainty in the measured pressure derivative. Once knowing the values of K_{T0} and $K_{T0}^{'}$, we can determine the pressure formulated with the isothermal compression component $P\ (V, T_0)$ along 300 K and the thermal pressure term $\Delta P_{th}(V, T)$as

$$P(V,T) = P(V,T_0) + \Delta P_{th}(V,T), \quad (1)$$

$P(V, T_0)$ is characterized by the third-order Birch-Murnaghan equation of state,[29]

$$P(V,T_0) = 3\varepsilon K_{T0}(1+2\varepsilon)^{5/2}[1 + 1.5\varepsilon(K_{T0}^{'} - 4)], \quad (2)$$

where

$$\varepsilon = 0.5[(V/V_0)^{-2/3} - 1], \quad (3)$$

and K_{T0} and $K_{T0}^{'}$ are the isothermal bulk modulus at ambient condition and its pressure derivative, respectively. The thermal pressure $\Delta P_{th}(V, T)$ can be evaluated by Mie-Grüneisen equation with the Debye model:

$$\Delta P_{th}(V,T) = \gamma \Delta E_{th}/V, \quad (4)$$

$$\Delta E_{th} = E_{th}(V,T) - E_{th}(V,T_0), \quad (5)$$

$$E_{th} = 9nRT\left(\frac{\theta}{T}\right)^{-3}\int_0^{\theta/T}\frac{x^3}{e^x - 1}dx, \quad (6)$$

$$\frac{\theta}{\theta_0} = \exp\left(\frac{\gamma_0 - \gamma}{q}\right) \quad (7)$$

$$\frac{\gamma}{\gamma_0} = \left(\frac{V}{V_0}\right)^q \quad (8)$$

where γ and θ are the Grüneisen parameter and the Debye temperature, respectively; and the constants n and R are the number of atoms per formula unit (n = 20) and the gas constant, respectively. According to the Eqs. (1)–(8) combined with previous publication data[13] of Grüneisen parameter $\gamma_0 = 1.15$ and dimensionless parameter $q = 1$, we can calculate pressures at different *P-T* conditions.

Fig. 5 shows x-ray density changes of polycrystalline pyrope garnet as a function of pressure and temperature determined form *in situ* x-ray diffraction measurements. The solid lines shows the polynomial fitting results based on the calculated densities, yielding a zero-pressure density of $\rho = 3.566$ (1) g/cm^3, which is in good agreement with earlier results of 3.57 and 3.56(2) by Sinogeikin and Bass[12] and Gwanmesia *et al.*,[8] respectively. The isothermal bulk modulus and its derivative derived from the compression data at room temperature ($K_{T0} = 169.2$ GPa, $K_{T0}^{'} = 4.35$) are consistent with previous studies by Zhang *et al.*[14] and Gwanmesia *et al.*,[8] respectively.

TABLE II. Elastic properties of polycrystalline $Mg_3Al_2(SiO_4)_3$ garnet, compared with previous studies.

Composition	K_{S0} (GPa)	G_0 (GPa)	$(\partial K_S/\partial P)_T$	$(\partial G/\partial P)_T$	$(\partial K_S/\partial T)_P$ (GPa/K)	$(\partial G/\partial T)_P$ (GPa/K)	Ref.
$Mg_3Al_2(SiO_4)_3$ garnet	170.0(2)	93.2(1)	4.51(2)	1.51(2)	−0.0170(1)	−0.0107(1)	This study
	171.2(11)	91.0(7)	4.55(20)	1.64(11)	−0.0206(15)	−0.0101(8)	Gwanmesia *et al.*[a]
	171(2)	92(1)	5.3(4)	1.6(2)	—	—	Chen *et al.*[b]
Majorite garnet	164.4(5)	94.9(2)	4.24(6)	1.11(3)	−0.0129(8)	−0.0103(4)	Irifune *et al.*[c]
$Mg_3Al_2(SiO_4)_3$ garnet	171(2)	94(2)	4.1(3)	1.3(2)	−0.0140(20)	−0.0092(10)	Sinogeikin *et al.*[d]
$Mg_4Si_4O_{12}$ garnet	166(3)	85(2)	4.2(3)	1.4(2)	—	—	Sinogeikin *et al.*[e]
$Mg_3Al_2(SiO_4)_3$ garnet	171(2)	—	4.4(2)	—	—	—	Zhang *et al.*[f]

[a]Ultrasonic interferometry (Refs. 8 and 9).
[b]Ultrasonic interferometry (Ref. 10).
[c]Ultrasonic interferometry (Ref. 32).
[d]Brillouin scattering (Refs. 11 and 12).
[e]Brillouin scattering (Ref. 11).
[f]Isothermal bulk modulus K_T and its pressure derivative $\partial K_T/\partial P$ from static compression (Ref. 14).

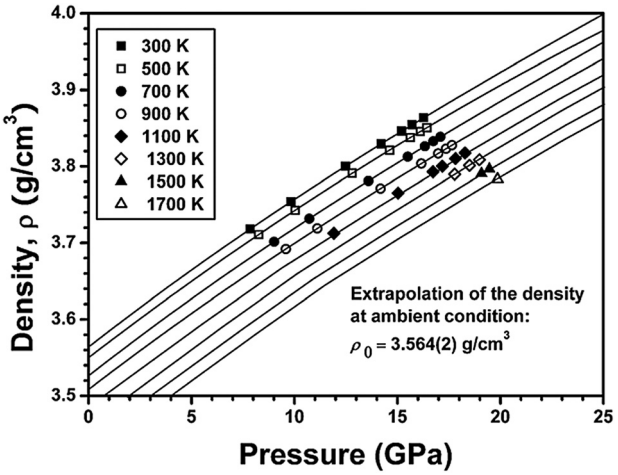

FIG. 5. X-ray density changes of polycrystalline pyrope garnet as a function of pressure and temperature determined form in situ x-ray diffraction measurements. The solid lines shows the polynomial fitting results based on the calculated densities, yielding a zero-pressure density of $\rho = 3.566(1)$ g/cm^3, which is in good agreement with earlier results of 3.57 and 3.56(2) by Sinogeikin and Bass (Ref. 12) and Gwanmesia *et al*. (Ref. 8), respectively.

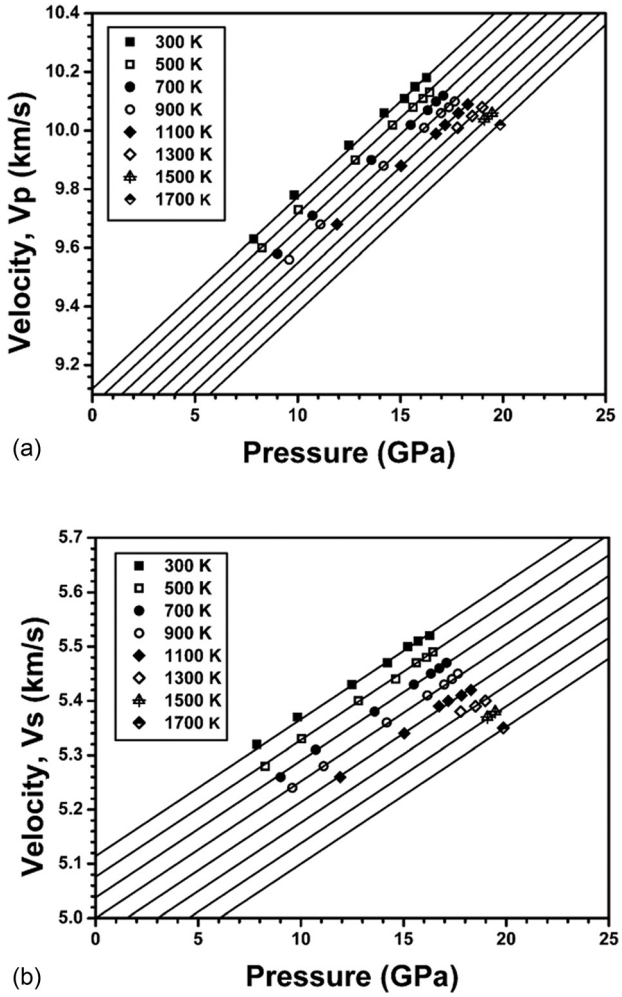

FIG. 6. (a) *P*-wave (*Vp*) and (b) *S*-wave (*Vs*) velocities of polycrystalline $Mg_3Al_2(SiO_4)_3$ pyrope garnet at high pressure and high temperature obtained from the present ultrasonic measurement. The solid lines are calculated from the two-dimensional (*P-T*) linear at entire *P-T* range.

Figs. 6(a) and 6(b) show *P*-wave (Vp) and S-wave (Vs) velocities of polycrystalline pyrope garnet changes in the present study as a function of pressure at different temperature, respectively. Both the *Vp* and *Vs* increase with increasing pressure and decrease with increasing temperature, whereas the temperature effect on *Vs* is larger than that on *Vp*. In addition, the present study shows a linear pressure and temperature dependence on both *Vp* and *Vs*, which behavior has also been observed in the recent study for grossular garnet,[30] but in contrast to the significantly non-linear temperature dependence of *Vs* observed for majorite with pyrolite composition using the same techniques.[31] This study suggests that non-linear behavior of elastic wave velocities (*Vp* and *Vs*) in pyrolite majorite is due to the complex mineral composition but not to the garnet structure itself. Two dimensional (*P-T*) linear fittings of *Vp* and *Vs* yield the equations $Vp = 9.119(6) + 0.0654(4) \times P - 0.00028(1) \times (T - 300)$, and $Vs = 5.114(3) + 0.0252(2) \times P - 0.00019(1) \times (T - 300)$, where *P* is the pressure in GPa and *T* is the temperature in K. As is known, the acoustic modes of lattice vibration are related to the compressional (*Vp*) and shear (*Vs*). Using the yield sound velocities data and the density of the garnet sample ($Vp = 9.119$ km/s, $Vs = 5.114$ km/s, $\rho = 3.566$ g/cm^3 at ambient conditions), we have determined the Debye temperature Θ_0 of 803 K, which is well consistent with the calculated data of Gwanmesia *et al*.[8] ($\Theta_0 = 804$ K) and Sinogeikin and Bass[11] ($\Theta_0 = 806$ K).

Figs. 7(a) and 7(b) show bulk (*Ks*) and shear (*G*) modulus of polycrystalline pyrope at high pressure and high temperature, which are derived from the velocities data, densities data in Table I. Bulk modulus (*Ks*) and shear modulus (*G*) also show linear pressure and temperature dependences at pressure up to 20 GPa and temperature up to 1700 K. Two dimensional (*P-T*) linear fittings of the present data on polycrystalline $Mg_3Al_2(SiO_4)_3$ garnet also yield the following parameters: $K_{S0} = 170.0$ (2) GPa, $\partial Ks/\partial P = 4.51(2)$, $\partial K_S/\partial T = -0.0170(1)$ GPa/K, $G_0 = 93.2(1)$ GPa, $\partial G/\partial P = 1.51(1)$, and $\partial G/\partial T = -0.0107(1)$ GPa/K, which is consistent with those of Gwanmesia *et al*.[8,9] within mutual uncertainties except for a significantly higher *G* and $\partial K_S/\partial T$ compared with those values of Gwanmesia *et al*.,[8,9] as summarized in Table II.

The bulk and shear modulus of the present study are also in good agreement with earlier results of Sinogeikin and Bass[11,12] and also agree with those of Chen *et al*.[10] within mutual uncertainties. The pressure dependences of bulk- and shear-modulus determined in this study, shown in Table II, are consistent with those of Gwanmesia *et al*.[8,9] Moreover, the adiabatic bulk modulus and its pressure derivative of this study are also consistent with the previous static compression experiment by Zhang *et al*.[14] Meanwhile, the pressure dependence of shear modulus *G* is consistent with the results by Gwanmesia *et al*.,[8,9] Chen *et al*.,[10] and Sinogeikin and Bass[11,12] within mutual uncertainties. However, the bulk modulus derivative for $\partial Ks/\partial P = 4.51(2)$ in this study is significantly lower than that of Chen *et al*.[10] ($\partial Ks/\partial P = 5.3$) and higher than that of Sinogeikin and Bass[11,12] ($\partial Ks/\partial P = 4.1$), respectively.

For experiments performed at room temperature,[10] the non-hydrostatic experimental condition or microstrain

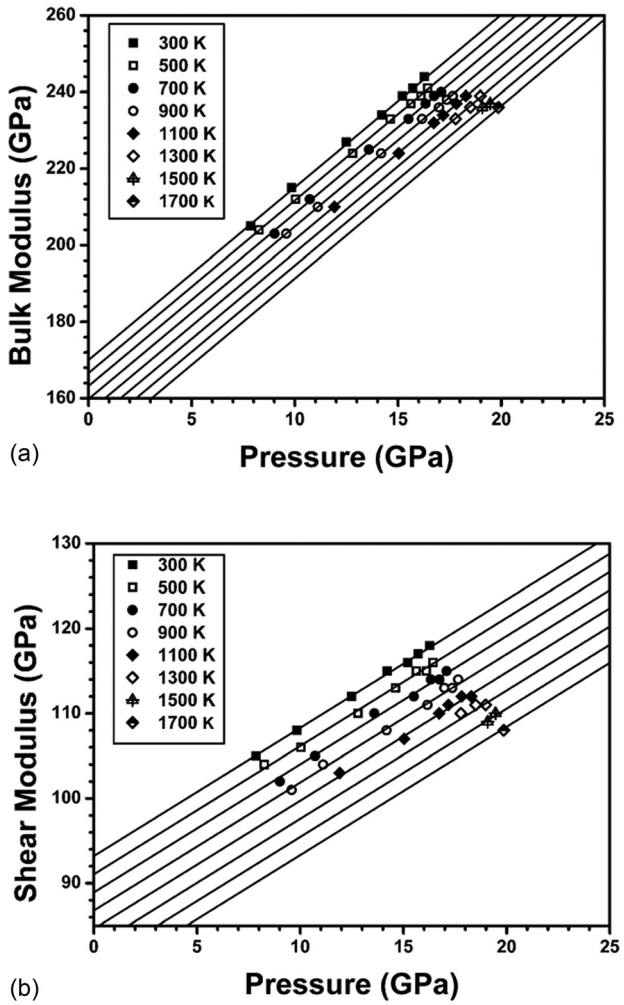

FIG. 7. (a) Bulk (Ks) and (b) shear (G) modulus of polycrystalline $Mg_3Al_2(SiO_4)_3$ pyrope at high pressure and high temperature obtained from the present ultrasonic measurement. The solid lines are calculated from the two-dimensional (P-T) linear at entire P-T range.

existed in a polycrystalline sample caused by grain-to-grain and/or grain-inside contact could affect its elastic properties, especially for the bulk modulus which is directly related to changes in the sample volume with pressure, as well as for its pressure derivative which is related to the changes in bulk modulus with pressure. Therefore, micro-stress in the sample may be responsible for the discrepancy between the present data and the previous study.[10] In addition, the relatively narrow pressure range for Gwanmesia *et al.*[8,9] (~9 GPa) and a pressure gradient greater than 1.6 GPa in a diamond anvil cell suggested by Sinogeikin and Bass[11] may be resulting in these discrepancies.[10–12] For understanding the mechanism of the effect of stress on the elastic properties and their derivative, further investigations are needed.

It is found that the temperature dependence of bulk modulus is consistent with that of Sinogeikin and Bass[11,12] within uncertainties but is slightly smaller than that of Gwanmesia *et al.*[8,9] In contrast, the temperature dependence of shear modulus agrees well with those of Gwanmesia *et al.*,[8,9] Sinogeikin and Bass,[11,12] respectively. Recent elasticity measurements indicated that the temperature dependence of Ks of garnets is around $-0.013 \sim -0.020$ (Table II). In contrast, temperature dependence of G is almost the same value, which suggests that composition dependence of $\partial G/\partial T$ is not observed in the present study.

Fig. 8 shows the changes of elastic wave velocities of polycrystalline pyrope garnet with temperature at some selected pressures in the middle to low parts of the mantle transition zone. For comparison, the corresponding variations for majorite with the pyrolite composition[31] using the same techniques is also shown in this figure. The present study shows a linear pressure and temperature dependence in both Vp and Vs, which is consistent with recent study on grossular by Kono *et al.*[30] and also agree with that of majorite in Vp by Irifune *et al.*[31] In contrast, Vs in majorite[31] shows more obvious nonlinear temperature dependence than that in pyrope of this study. Our study suggests the linear behaviors of sound velocities depend on the mineral composition but not for all the minerals. Thus, the sound velocity measurements of the effects of the cations such as Al, Na, and Fe on the mantle garnet as well as other minerals, at P-T conditions up to the mantle transition region, are needed to further constrain the composition and the constitution of the mantle transition region.

Based on the present experimental data, we have also calculated the Young's modulus E and Poisson's ratio ν by applying $E = \rho Vs(3Vp^2 - 4Vs^2)/(Vp^2 - Vs^2) = 9KG/(3K + G)$ and $\nu = (3K - 2G)/(6K + 2G)$, respectively, as shown in Table III. For comparison, elastic properties of $Y_3Al_2(AlO_4)_3$ garnet as well as some typical materials in MgO-Al_2O_3-SiO_2 system from previous studies[26,33–38] are also shown in Table III. The crystallographic structure of garnets has been formulated as $X_3Y_2(ZO_4)_3$, where X, Y, and Z atoms occupy dodecahedral, octahedral, and tetrahedral crystallographic sites, respectively. This feature makes the garnet structure flexible in accommodating a variety of cations. Besides silicon, a large number of elements have been put on the Z site, including Ge, Ga, Al, V, and Ti. $Y_3Al_2(AlO_4)_3$ (YAG) garnet, as the same

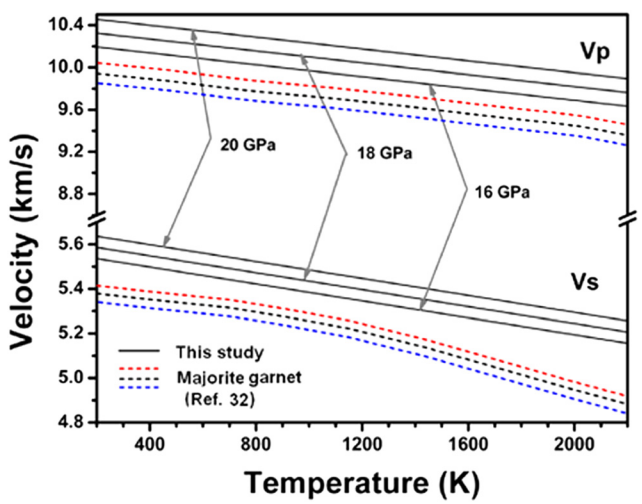

FIG. 8. Compressional (P-) and shear (S-) wave velocities changes of polycrystalline $Mg_3Al_2(SiO_4)_3$ pyrope garnet as a function of temperature at some representative pressures in the mantle transition region. The solid lines show the P- and S-wave velocities obtained from the present study, while the dashed lines represent those based on recent study by Irifune *et al.* (Ref. 31).

TABLE III. Elastic properties of polycrystalline $Mg_3Al_2(SiO_4)_3$ garnet and $Y_3Al_2(AlO_4)_3$ garnet as well as some typical materials in MgO-Al_2O_3-SiO_2 system from previous studies.

Materials/Compounds	Bulk modulus K (GPa)	Shear modulus G (GPa)	Young's modulus[a] E (GPa)	Poisson's ratio[b] ν	Ref.
$Mg_3Al_2(SiO_4)_3$-garnet	170.0	93.2	236.4	0.27	This study
$Y_3Al_2(AlO_4)_3$-garnet	179	112	278.0	0.24	Marquardt *et al.*[c]
MgO-periclase	162.5	130.4	308.6	0.18	Zha *et al.*[d]
Y_2O_3-yttria	150	66.3	173.4	0.31	Palko *et al.*[e]
α-Al_2O_3	252.1	161.3	398.9	0.24	Wdowik *et al.*[f]
α-SiO_2	40.3	45.1	98.5	0.09	Yao *et al.*[g]
SiO_2-stishovite	305	217	526.2	0.21	Li *et al.*[h]
$MgAl_2O_4$-spinel	197.9	110	275	0.27	Yoneda and Zou *et al.*[i]

[a]Calculated Young's modulus E (GPa) based on the references therein.
[b]Calculated Poisson's ratio ν based on the references therein.
[c]Brillouin scattering (Ref. 32).
[d]X-ray diffraction and Brillouin scattering (Ref. 26).
[e]Brillouin scattering (Ref. 33).
[f]Theoretical calculation (Ref. 34).
[g]Theoretical calculation (Ref. 35).
[h]Ultrasonic interferometry (Ref. 36).
[i]Data from Refs. 37 and 38.

structure with $Mg_3Al_2(SiO_4)_3$ garnet, shows comparative elastic properties as that of $Mg_3Al_2(SiO_4)_3$ garnet. The elasticity differences should be due to the different ionic radii of Mg^{2+} and Y^{3+}, Si^{4+} and Al^{3+}, resulting in the different size of AlO_4 and SiO_4 tetrahedra. As seen from Table III, substitution of Y^{3+}, Al^{3+} for Mg^{2+}, Si^{4+} in the X and Z sites will decrease the bulk modulus, shear modulus, and Young's modulus, in contrast to an increase of the Poisson's ratio from 0.24 to 0.27. The present experimental data may be applied to develop composition-systematic relations to predict the high-pressure elasticity of all the garnet end members, garnet solid solutions as well as for some related materials. Therefore, understanding the elastic properties and/or sound velocities of $Mg_3Al_2(SiO_4)_3$ garnet gives some great implications for other garnets such as $Y_3Al_5O_{12}$ and $Y_3Fe_5O_{12}$ seeing from the solid state reactions $3MgO + Al_2O_3 + 3SiO_2 \rightarrow Mg_3Al_2(SiO_4)_3$ and $3Y_2O_3 + 5(Fe,Al)_2O_3 \rightarrow 2Y_3(Fe,Al)_5O_{12}$.

IV. CONCLUSIONS

Polycrystalline $Mg_3Al_2(SiO_4)_3$ pyrope sample has been synthesized at 11 GPa and 1200 °C for 1.5 h from homogeneous glass. Sound velocities for synthetic polycrystalline pyrope were measured at pressures up to 20 GPa and temperatures of 300–1700 K, equivalent to the P-T conditions of the middle part of the mantle transition zone. The present data show a linear pressure and temperature dependence in both Vp and Vs, which is in contrast to the significantly nonlinear temperature dependence of majorite garnet with the pyrolite composition by Irifune *et al.*[31] This study combined with previous studies suggests that non-linear behavior of sound velocities depend on the mineral composition but not for all the minerals or the crystal structure. In addition, the present data, together with previous studies on pyrope garnet by Gwanmesia *et al.*[8,9] and Sinogeikin and Bass,[11,12] provide a compatible data set for constructing a more comprehensive mineralogical model for the transition zone of the Earth mantle and also provide some implications for high-pressure elasticity study for other garnets such as $Y_3Al_2(AlO_4)_3$ (YAG) and $Y_3Fe_2(FeO_4)_3$ (YIG) as well as for some related materials/minerals in MgO-Al_2O_3-SiO_2 system.

ACKNOWLEDGMENTS

This research was supported by the Global-COE program "Deep Earth Mineralogy." The authors thank N. Nishiyama, Y. Tange, and F. Wang for their assistance in this experiment on BL04B1 at SPring-8 (Proposal No. 2011A0082). We also acknowledge G. D. Gwanmesia, B. Li, Y. Kono, and T. Inoue for the valuable discussion and suggestions.

[1]G. S. Corman, J. Mater. Sci. Lett. **12**, 379 (1993).
[2]R. Kolesov, Phys. Rev. A **76**, 43831 (2007).
[3]L. Wen, X. Sun, Z. Xiu, S. Chen, and C. T. Tsai, J. Eur. Ceram. Soc. **24**, 2681 (2004).
[4]D. L. Anderson and J. D. Bass, Geophys. Res. Lett. **11**, 637, doi: 10.1029/GL011i007p00637 (1984).
[5]T. Irifune and A. E. Ringwood, Earth Planet. Sci. Lett. **86**, 365 (1987).
[6]M. Akaogi, "Phase transitions of minerals in the transition zone and upper part of the lower mantle," in *Advances in High-Pressure Mineralogy*, edited by E. Ohtani (Geological Society of America, 2007), pp. 1–13.
[7]F. Jiang, S. Speziale, S. R. Shieh, and T. S. Duffy, J. Phys.: Condens. Matter **16**, S1041 (2004).
[8]G. D. Gwanmesia, J. Zhang, K. Darling, J. Kung, B. Li, L. Wang, D. Neuville, and R. C. Liebermann, Phys. Earth Planet. Inter. **155**, 179 (2006).
[9]G. D. Gwanmesia, I. Jackson, and R. C. Liebermann, Phys. Chem. Miner. **34**, 85 (2007).
[10]G. Chen, J. A. Cooke, G. D. Gwanmesia, and R. C. Liebermann, Am. Mineral. **84**, 384 (1999).
[11]S. V. Sinogeikin and J. D. Bass. Phys. Earth Planet. Inter. **120**, 43 (2000).
[12]S.V. Sinogeikin and J. D. Bass, Earth Planet. Sci. Lett. **203**, 549 (2002).
[13]Y. Wang, D. J. Weidner, J. Zhang, G. D. Gwanrnesia, R. C. Liebermann, and J. D. Bass, Phys. Earth Planet. Inter. **105**, 59 (1998).
[14]L. Zhang, H. Ahsbahs, and A. Kutoglu, Phys. Chem. Miner. **25**, 301 (1998).
[15]P. G. Conrad, C. S. Zha, H. K Mao, and R. J. Hemley, Am. Mineral. **84**, 374 (1999).
[16]K. Hirose, Y. Fei, S. Ono, T. Yagi, and K. Funakoshi, Earth Planet. Sci. Lett. **184**, 567 (2001).

[17]G. D. Gwanmesia, R. C. Liebermann, and F. Guyot, Geophys. Res. Lett. **17**, 1331 (1990).
[18]Y. Higo, T. Inoue, T. Irifune, K. Funakoshi, and B. Li, Phys. Earth Planet. Inter. **166**, 167 (2008).
[19]Y. Kono, T. Irifune, Y. Higo, T. Inoue, and A. Barnhoorn, Phys. Earth Planet. Inter. **183**, 196 (2010).
[20]B. Li, G. Chen, R. C. Liebermann, and D. J. Weidner, Science, **281**, 675 (1998).
[21]J. Kung, B. Li, T. Uchda, Y. Wang, D. Neuville, and R. C. Liebermann, Phys. Earth Planet. Inter. **147**, 27 (2004).
[22]B. Li and J. Zhang, Phys. Earth Planet. Inter. **151**, 143 (2005).
[23]B. Li, K. Chen, J. Kung, R. C. Liebermann, and D. J. Weidner, J. Phys.: Condens. Matter **14**, 11337 (2002).
[24]B. Li, J. Kung, and R. C. Liebermann, Phys. Earth Planet. Inter. **143–144**, 559 (2004).
[25]J. Kung, B. Li, D. J. Weidner, J. Zhang, and R. C. Liebermann, Earth Planet. Sci. Lett. **203**, 557 (2002).
[26]C. S. Zha, H. K. Mao, and R. J. Hemley, Proc. Natl. Acad. Sci. U.S.A. **97**, 13494 (2000).
[27]W. Liu, J. Kung, B. Li, N. Nishiyama, and Y. Wang, Phys. Earth Planet. Inter. **174**, 98 (2009).
[28]G. F. Davies and A. M. Dziewonski, Phys. Earth Planet. Inter. **10**, 336 (1975).
[29]F. Birch, J. Geophys. Res. **57**, 227, doi: 10.1029/JZ057i002p00227 (1952).
[30]Y. Kono, S. Gréaux, Y. Higo, H. Ohfuji, and T. Irifune, J. Earth Sci. **21**, 782 (2010).
[31]T. Irifune, Y. Higo, T. Inoue, Y. Kono, H. Ohfuji, and K. Funakoshi, Nature (London) **451**, 814 (2008).
[32]H. Marquardt, S. Speziale, S. Jahn, S. Ganschow, and F. R. Schilling, J. Appl. Phys. **106**, 093519 (2009).
[33]J. W. Palko, W. M. Kriven, S. V. Sinogeikin, J. D. Bass, and A. Sayir, J. Appl. Phys. **89**, 7791 (2001).
[34]U. D. Wdowik, K. Parlinski, and A. Siegel, J. Phys. Chem. Solids **67**, 1477 (2006).
[35]H. Yao, L. Ouyang, and W. Y. Ching, J. Am. Ceram. Soc. **90**, 3194 (2007).
[36]B. Li, S. M. Rigdenb, and R. C. Liebermann, Phys. Earth Planet. Inter. **99**, 113 (1996).
[37]Y. Zou, D. He, X. Wei, R. Yu, T. Lu, X. Chang, S. Wang, and L. Lei, Mater. Chem. Phys. **123**, 529 (2010).
[38]A. Yoneda, J. Phys. Earth **38**, 19 (1990).